Effect of Sphingomyelin Headgroup Size on Molecular Properties and Interactions with Cholesterol

Anders Björkbom,[†*] Tomasz Róg,[§¶] Karol Kaszuba,[§‖] Mayuko Kurita,[‡] Shou Yamaguchi,[‡] Max Lönnfors,[†] Thomas K. M. Nyholm,[†] Ilpo Vattulainen,[§¶**] Shigeo Katsumura,[‡] and J. Peter Slotte[†]

[†]Department of Biosciences, Åbo Akademi University, Turku, Finland; [‡]School of Science and Technology, Kwansei Gakuin University, Sanda City, Japan; [§]Department of Physics, Tampere University of Technology, Tampere, Finland; [¶]Department of Applied Physics, Aalto University of Science and Technology, Espoo, Finland; [‖]Department of Physics and Biophysics, University of Warmia and Mazury, Olsztyn, Poland; and [**]MEMPHYS Center for Biomembrane Physics, University of Southern Denmark, Odense, Denmark

ABSTRACT   Sphingomyelins (SMs) and sterols are important constituents of the plasma membrane and have also been identified as major lipid components in membrane rafts. Using SM analogs with decreasing headgroup methylation, we systemically analyzed the effect of headgroup size on membrane properties and interactions with cholesterol. An increase in headgroup size resulted in a decrease in the main phase transition. Atom-scale molecular-dynamics simulations were in agreement with the fluorescence anisotropy experiments, showing that molecular areas increased and acyl chain order decreased with increasing headgroup size. Furthermore, the transition temperatures were constantly higher for SM headgroup analogs compared to corresponding phosphatidylcholine headgroup analogs. The sterol affinity for phospholipid bilayers was assessed using a sterol-partitioning assay and an increased headgroup size increased sterol affinity for the bilayer, with a higher sterol affinity for SM analogs as compared to phosphatidylcholine analogs. Moreover, the size of the headgroup affected the formation and composition of cholesterol-containing ordered domains. Palmitoyl-SM (the largest headgroup) seemed to attract more cholesterol into ordered domains than the other SM analogs with smaller headgroups. The ordering and condensing effect of cholesterol on membrane lipids was also largest for palmitoyl-SM as compared to the smaller SM analogs. The results show that the size of the SM headgroup is crucially important for SM-SM and SM-sterol interactions. Our results further emphasize that interfacial electrostatic interactions are important for stabilizing cholesterol interactions with SMs.

INTRODUCTION

Biomembranes are composed of a vast variety of membrane lipids and proteins, and exhibit functionally dependent variations in composition among the cell compartments (1). These differences in lipid composition have been shown to affect membrane lipid organization in the lateral plane of the membrane (1–5). Sphingomyelins (SMs) and cholesterol have been shown to form lateral domains, highlighting phase separation from unsaturated phosphatidylcholines (PCs) in model membrane systems that resemble the composition of plasma membranes (2,6,7). Dynamically, in the plasma membrane of living cells, the lateral diffusion of sphingolipids and glycosylphosphatidylinositol-anchored proteins has also been shown to be slowed down by cholesterol (3). The effects of cholesterol on lateral diffusion have been explained by the existence of short-lived nanoscopic lateral domains, transiently trapping sphingolipids, and glycosylphosphatidylinositol-anchored proteins (3). Such membrane domains, rich in cholesterol and sphingolipids, are commonly called lipid rafts, although their exact definition is still a matter of discussion (8). Originally, lipid rafts (9) were proposed to serve as a sorting mechanism during sphingolipid and protein transport (10). Currently, membrane rafts are defined as "small (10–200 nm), heterogeneous, highly dynamic, sterol- and

sphingolipid-enriched domains that compartmentalize cellular processes" (8). Taking into account the above-mentioned studies and several others (5,11), it appears that lateral heterogeneities, comparable to the concept of membrane rafts, have been identified both in living cells and in compositionally simpler model membrane systems. However, the mechanisms underlying the formation of lateral lipid heterogeneities are not fully understood at a molecular level.

Many factors arising from the large structural differences among phospholipids, such as acyl chain length (12,13), acyl chain unsaturation/branching (12,14–17), hydrogen (H)-bonding/charge-pairing functions at the membrane-water interface (18–21), and headgroup size (22), are known to affect their interactions with cholesterol. The sphingolipid structure allows for H-bonding at the membrane-water interface, owing to the C_2 amide linkage and the C_3 hydroxyl group in the sphingosine backbone (Fig. 1) (23). Atomistic molecular-dynamics (MD) simulations have shown intramolecular H-bonding between the C_3 hydroxyl group and the phosphate oxygens in SM headgroups. H-bonding has also been shown to increase headgroup tilt and thus the effective area of the phosphocholine headgroup in SM bilayers (23).

It is thus likely that the headgroup size and interactions in the headgroup region affect interactions between phospholipids and cholesterol. Currently, several models describe cholesterol-phospholipid interactions at a molecular level,
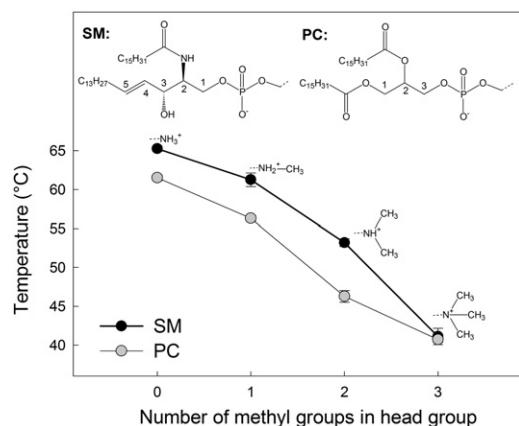
FIGURE 1 Chemical structures of headgroup analogs and their gel-to-fluid-phase transition temperatures (T_m) as reported by the anisotropy of DPH.

including the umbrella model (24,25), the condensed complex model (26), and the superlattice model (27). In the umbrella model, the phospholipid headgroup is assumed to shield the hydrophobic region of cholesterol from unfavorable interactions with water (24). However, since phospholipid/phospholipid and phospholipid/cholesterol interactions are affected by so many different variables (e.g., acyl chain length, unsaturation, headgroup properties, and the presence of competing colipids), no single interaction model is sufficient to fully explain how lipid interactions are governed.

The effects of phospholipid headgroup size on membrane properties have previously been studied using saturated PC analogs with varying headgroup methylation (28–31). Although SMs and PCs have the same phosphocholine headgroup, they differ greatly in their interfacial structure (Fig. 1). Because the plasma membrane contains high levels of SMs, it is critically important to directly study interactions between these lipids and cholesterol. In this work, we used SM analogs varying in headgroup methylation to study how the size of the SM headgroup affects the molecular properties of SMs and interactions with cholesterol, using fluorescence spectroscopy and atomistic MD simulations. We also compared our results obtained with SM headgroup analogs with corresponding PC headgroup analogs. The results show that an increase in headgroup size increased sterol affinity for bilayer membranes. An increase in headgroup size also led to a larger amount of cholesterol in ordered domains, as well as to an increased ordering and condensing effect of cholesterol on the acyl chains. We also found that the SM analogs had a higher gel-to-fluid-phase transition temperature (T_m) and higher sterol partitioning coefficients as compared to corresponding PC analogs. The results emphasize the important effect of SM headgroup size on SM-SM and SM-sterol interactions, and demonstrate how the structural differences between SMs and PCs manifest themselves as key differences in interactions with

cholesterol, resulting in major alterations in membrane properties.

MATERIALS AND METHODS

N-palmitoyl ceramide phosphoethanolamine (CPE), *N*-palmitoyl ceramide phosphoethanolamine-N-methyl (CPE-Me), and *N*-palmitoyl ceramide phosphoethanolamine-N,N-dimethyl (CPE-Me$_2$) were synthesized, and *N*-palmitoyl-sphingomyelin (PSM) was purified and identified as described in the Supporting Material. For simplicity, we call these four sphingosine-based headgroup analogs SM analogs. The corresponding glycerol-based headgroup (1,2-dipalmitoyl-*sn*-glycero-3-phosphoethanolamine (DPPE), 1,2-dipalmitoyl-*sn*-glycero-3-phosphoethanolamine-N-methyl (DPPE-Me), 1,2-dipalmitoyl-*sn*-glycero-3-phosphoethanolamine-N,N-dimethyl (DPPE-Me$_2$), and 1,2-dipalmitoyl-*sn*-glycero-3-phosphocholine (DPPC)) analogs are called PC analogs. For the sources of the commercial chemicals and a description of the synthetic procedures used, see the Supporting Material.

The steady-state anisotropy of 1,6-diphenyl-3,5-hexatriene (DPH) was measured to determine the T_m for all lipids. The partitioning of cholesta-5,7,9(11)-trien-3-β-ol (CTL) between large unilamellar vesicles and methyl-β-cyclodextrin (mβCD) was measured to determine the affinity of the sterol for the bilayers containing the headgroup analogs. The partitioning coefficient was calculated as described previously (32). Vesicles for partitioning studies were composed of 1-palmitoyl-2-oleoyl-*sn*-glycero-3-phosphocholine (POPC)/headgroup analog, (8:2 molar ratio) with 2 mol % CTL. Fluorescence quenching of the sterol analog CTL by 1-palmitoyl-2-stearoyl-(7-doxyl)-*sn*-glycero-3-phosphocholine (7SLPC) was measured to study the formation and melting of sterol-containing ordered domains. The anisotropy of *trans*-parinaric acid (*t*Pa) was further used to study ordered domain formation and melting independently of their sterol content. The lipid composition in the quenching assay and *t*Pa anisotropy experiments was POPC/headgroup analog/sterol (60:30:10, molar ratio), and in the F-sample in the quenching assay, 7SLPC replaced 50 mol % of POPC. MD simulations were performed on systems composed of pure SM analogs and SM analog/cholesterol (8:2 molar ratio) systems to study interactions at an atomistic level. Additional details for all methods are given in the Supporting Material.

RESULTS

Anisotropy of DPH

To analyze how the headgroup size of SM affects T_m, we measured the anisotropy of DPH in one-component bilayers for all headgroup analogs (Fig. 1). The anisotropy of DPH reported a clear correlation between T_m and headgroup size for both SM and PC analogs. An increase in headgroup size resulted in a decrease in T_m. The T_m-values of the SM analogs (CPE (65.3°C), CPE-Me (61.3°C), and CPE-Me$_2$ (53.2°C)) were constantly higher than the corresponding T_m-values for PC analogs (DPPE (61.5°C), DPPE-Me (56.3°C), and DPPE-Me$_2$ (46.3°C)), indicating stronger interactions between the sphingosine-based lipids in the gel phase. The results are in good agreement with previously reported T_m-values for PC analogs, PSM, and CPE (22,33).

Sterol affinity for bilayers containing headgroup analogs

The sterol affinity for unilamellar bilayer vesicles (Fig. 2) was assessed by measuring the equilibrium distribution of
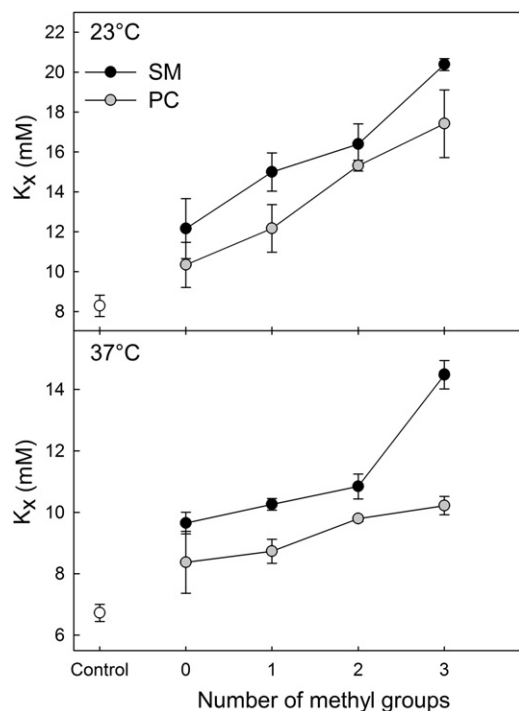
FIGURE 2 Sterol affinity for bilayer membranes as measured by the equilibrium distribution of CTL between mβCD and unilamellar bilayer vesicles. The vesicles were composed of POPC/headgroup analog (8:2, molar ratio) for SM analogs (*black*) and PC analogs (*gray*), as well as only POPC (*white*) at 23°C (*upper panel*) and 37°C (*lower panel*).

the fluorescent cholesterol analog CTL between mβCD and vesicles containing 80 mol % of a fluid matrix lipid (POPC) and 20 mol % headgroup analog (32). The results showed a clear correlation between headgroup size and sterol affinity for bilayer vesicles containing SM or PC analogs at both 23°C and 37°C. An increase in headgroup size increased sterol affinity for bilayer vesicles. It is noteworthy that sterol affinity at 37°C was noticeably higher for PSM-containing vesicles as compared to all other analogs, indicating highly favorable sterol-PSM interactions at physiological temperature. Furthermore, the sterol affinity was constantly higher for bilayer vesicles containing SM analogs than for corresponding PC analogs.

All saturated headgroup analogs increased sterol affinity for the bilayer vesicles as compared to the fluid matrix lipid POPC. Sterol affinity for the vesicles was also always higher at 23°C than at 37°C. The increased sterol affinity for the bilayer vesicles containing any of the saturated analogs, and the increased sterol affinity at lower temperature show that membrane order had a general increasing effect on sterol affinity for bilayer vesicles. An increase in headgroup size, however, markedly increased the sterol affinity, showing an inverse correlation with the gel-phase stability of the SM analogs.

Formation and melting of ordered domains in three-component bilayer vesicles

We further characterized the effects of headgroup methylation on cholesterol interactions by studying the formation and subsequent melting of sterol-containing ordered domains in ternary model systems using fluorescence quenching of CTL by the quencher 7SLPC (Fig. 3, *left panels*) (2). As a result of the bulky doxyl group, 7SLPC will have a strong preference for the liquid disordered phase and be separated from CTL in the presence of sterol-containing ordered domains (2). The introduction of varying substituents at the center of the acyl chains of PCs has been shown to markedly decrease the T_m and thus fluidize the PC molecule (34). A temperature-induced melting of the ordered domains results in increased quenching of CTL fluorescence as it comes in contact with 7SLPC. To correct for the direct temperature-induced decrease in fluorescence intensity of CTL, the F/F_0 ratio is calculated, with the F_0 sample lacking quencher. The F/F_0 ratio shows the amount of CTL fluorescence that is protected from quenching (ordered domain existence) as a function of temperature (2). The phase state of the SM analog-containing ordered domains is gel-like, liquid-ordered, or a combination thereof, depending on the temperature. The POPC/PSM/cholesterol (60:30:10, molar ratio) composition is very close to the three-phase region at 23°C, whereas no gel phase is present at 37°C (see phase diagrams in de Almeida et al. (35) and Halling et al. (36)). For the other SM and PC analogs, the relative amount of gel-like or liquid-ordered domain is not known. The formation and relative sterol content of ordered domains was clearly affected by the size of the headgroup. Among the SM analogs, PSM formed domains that clearly contained more sterol as compared to analogs with smaller headgroups. The sterol content can be evaluated for either SM or PC analogs by comparing the F/F_0 amplitude (the relative amount of CTL initially shielded from quenching but subsequently quenched after melting) of the domain melting. CPE-Me and CPE formed ordered domains containing small amounts of sterol, whereas no sterol-containing ordered domains could be observed for CPE-Me$_2$. The failure of CPE-Me$_2$ to form sterol-containing ordered domains could possibly be explained by their small size (inefficient quenching protection) or by packing properties that make CTL (and sterol) miscibility unfavorable (see Discussion). Among the PC analogs, both DPPC and DPPE-Me$_2$ formed sterol-containing ordered domains, with the DPPC domains containing slightly more sterol. No sterol-containing ordered domains were observed in bilayers containing DPPE-Me or DPPE as the saturated phospholipid.

We further studied the properties of ordered domains by measuring the anisotropy of *t*Pa in ternary bilayers (Fig. 3, *right panels*). *t*Pa has been shown to preferentially partition into ordered lipid phases (37), and melting of ordered domains was observed from the overall decrease in
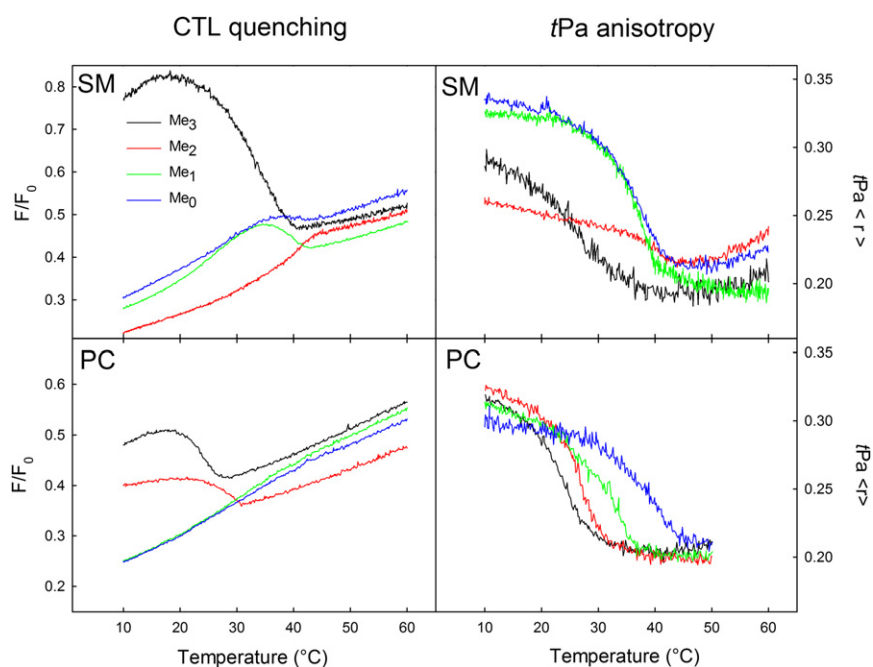
FIGURE 3 Existence and subsequent melting of ordered domains in an otherwise fluid lipid matrix. Headgroup-dependent formation of sterol-containing ordered domains was studied using fluorescence quenching of the cholesterol analog CTL by the quencher 7SLPC (*left panels*). The anisotropy of *t*Pa (*right panels*) was further used to study the melting of ordered domains, not necessarily containing sterol. The color scheme depicts the size of the headgroup according to Me_3 (*black*), Me_2 (*red*), Me_1 (*green*), and Me (*blue*) for SM analogs (*upper panels*) and PC analogs (*lower panels*). Samples consisted of POPC/headgroup analog/cholesterol (60:30:10, molar ratio), and in the CTL quenching study, 7SLPC replaced 50 mol % of POPC in the fluid matrix of the F-sample.

anisotropy of *t*Pa as a function of temperature. In contrast to the fluorescence quenching of CTL, the anisotropy of *t*Pa measures melting of ordered domains independently of their cholesterol content. As observed from the sharp decrease in anisotropy of *t*Pa, all headgroup analogs formed gel-like ordered domains. With the exception of $CPE-Me_2$, the ordered domains melted in a headgroup size-dependent manner. A larger headgroup caused the ordered domains to melt at lower temperatures as compared to domains containing smaller headgroup analogs. Among the SM analogs, CPE-Me and CPE analogs had higher *t*Pa anisotropies below the domain melting temperature as compared to PSM, whereas $CPE-Me_2$ had a lower *t*Pa anisotropy below the domain melting temperature. In agreement with the lack of formation of sterol-containing domains for $CPE-Me_2$, the lower anisotropy observed for $CPE-Me_2$ could indicate that *t*Pa failed to incorporate into the $CPE-Me_2$-rich domain because of unusual lateral packing properties (see Discussion). The possibility that $CPE-Me_2$ formed a liquid-crystalline phase was excluded on the basis of DSC data (Fig. S2) and additional *t*Pa anisotropy experiments (Fig. S3). The DSC and additional *t*Pa anisotropy results showed that $CPE-Me_2$ formed a gel phase that was problematic to detect with *t*Pa. In analogy, the higher anisotropies for CPE-Me and CPE are most likely due to tightly packed, gel-like ordered domains that decrease the movement of (but do not exclude) the *t*Pa molecule.

Structural order in SM analog bilayers

To further study the molecular properties of headgroup modified SM analogs, we conducted atomistic MD simula-tions on systems composed of SM analogs and SM analog/cholesterol (8:2, molar ratio) mixtures (for a description of the MD analysis, see the Supporting Material). We found that the average area per molecule was smallest for CPE and increased with increasing numbers of methyl groups on the headgroup nitrogen (Fig. 4 A). As an increasing molecular area reflects increasing membrane fluidity, this trend is in line with the observed T_m-values. This in turn is in agreement with findings for other lipid bilayer systems (38) that have shown an inverse relation between the area per lipid and T_m. As for the effect of cholesterol, its addition was found to decrease the area per phospholipid in all of the systems due to the well-known condensing effect of cholesterol (Fig. 4 A). However, it is noteworthy that the effect was most prominent in systems with a larger number of methyl groups.

The mean values of the deuterium order parameter (S_{CD}), averaged over the saturated segments of the sphingosine tail, are shown in Fig. 4 C. As expected from the results for the average area per lipid, the highest order was observed for CPE and the lowest one for PSM. In all cases, cholesterol increased the order parameter. The effect became stronger as the number of methyl groups increased. Profiles of S_{CD} along the sphingosine and acyl chains are shown in Fig. S4. Values of membrane thickness in terms of the phosphate-to-phosphate (P-P) distance (Fig. 4 B) show that membrane thickness was inversely proportional to the average area per lipid and proportional to the average acyl chain order.

Previous studies have shown that the tilt of a sterol can indicate its overall ordering effect on membrane phospholipids, and that it is sensitive to modifications in sterol structure and lipid unsaturation (39). However, this study the tilt
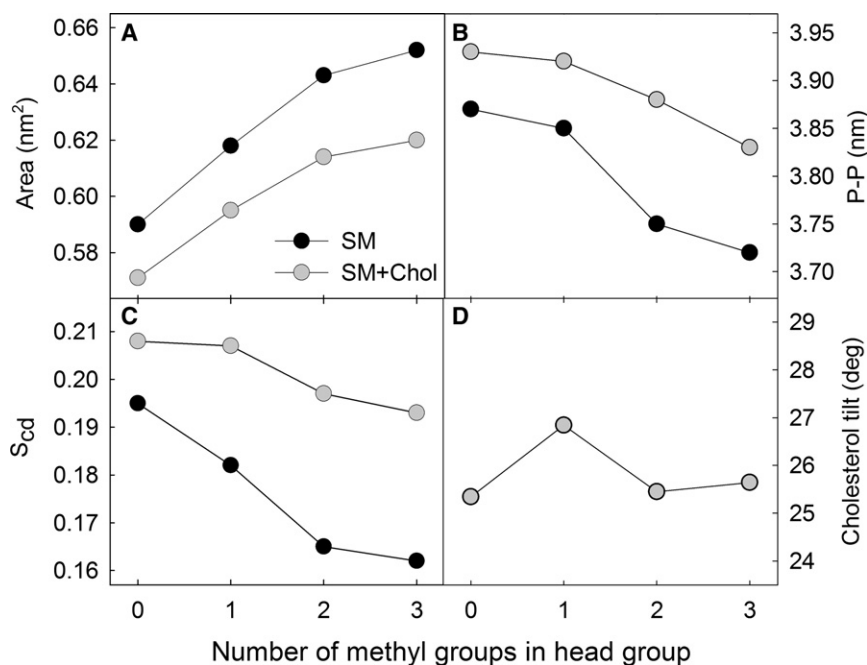
FIGURE 4 Membrane properties of SM analogs. (*A*) Area per lipid molecule (cholesterol excluded). (*B*) Membrane thickness measured as phosphate-phosphate (P-P) distance. (*C*) Order parameter S_{CD} averaged over the sphingosine chain. (*D*) Tilt of cholesterol molecule as measured from the (outgoing) bilayer normal. The simulated systems were composed of pure SM analogs and SM analogs with 20 mol % cholesterol.

values (Fig. 4 *D*) were found to be largely identical. The structural changes in the headgroup region apparently did not affect cholesterol tilt. Hence, the observed changes in area per lipid were due not only to cholesterol's ordering capability but also to packing in the headgroup region.

Interactions at the water-membrane interface for SM analogs

The systems analyzed here contain a set of functional groups that are capable of participating in both H-bonds and charge pairs. First, there are three functional groups in the sphingosine moiety (Fig. 1): a carbonyl group that can act as an H-bond acceptor, a hydroxyl group that can act as both donor and acceptor, and an amide group that acts mostly as a donor in H-bonding. These functional groups are in the region where the hydroxyl group of cholesterol is located (shown in the density profiles in Fig. S5). Next, there are phosphate groups that can serve as H-bond acceptors and are located deeper in the water phase compared to the previous three functional groups. The final groups are choline and amine, as well as the two intermediates, which are mostly in the water phase. The choline group participates in the above-mentioned charge pairs, whereas the amine group is an H-bond donor. The two intermediate groups can participate in both charge pairing and H-bonding because they have N-H and N-CH$_3$ groups whose charge distribution is similar to the native molecules.

First we analyzed the interactions between cholesterol and SM analogs. The numbers of H-bonds and charge pairs are given in Table 1. As we gradually replaced hydrogens in the amine group with methyl groups, the number of H-bonds

between the cholesterol and lipids decreased. This decrease concerned mainly H-bonds in which cholesterol acts as an acceptor (OH and NH groups). At the same time, the number of H-bonds in which cholesterol acts as a donor (OP and OC) increased slightly. However, the overall decrease in the number of H-bonds was compensated for by an increasing number of charge pairs. This explains why there was a decrease in the number of H-bonds in which cholesterol acted as an acceptor: these bonds were replaced by more favorable charge pairs. Further, the number of charge pairs not only compensated for the lost H-bonds but also led to an increase in the total number of intermolecular interactions (by >20% when we compared the CPE-cholesterol with the PSM-cholesterol bilayer). Next we analyzed interactions between cholesterol and

TABLE 1 Interactions of cholesterol with SM analogs and water

| H-bonding partner for Chol | CPE | SM analogs | | PSM |
		CPE-ME	CPE-ME$_2$	
OH	0.61	0.38	0.37	0.33
OC	0.22	0.26	0.27	0.28
NH	0.17	0.13	0.11	0.09
OP	0.06	0.11	0.09	0.10
NH (in headgroup)	0.02	0.05	0.03	-
Total H-bond	1.08	0.93	0.87	0.81
Charge pairs	-	0.18	0.33	0.52
Total lipid interactions	1.08	1.11	1.20	1.33
H-bonds with H$_2$O	0.94	1.00	1.04	0.99

Number of intermolecular H-bonds and charge pairs between cholesterol and SMs/water in systems composed of SM analogs with 20 mol % cholesterol. Errors are <0.01.

water (Table 1). The number of H-bonds was about one per cholesterol in all cases. In CPE-Me$_2$ the number of water molecules bonded to cholesterol was largest (~5% larger than in CPE-Me and PSM). This suggests that the CPE-Me$_2$ group is the least efficient at shielding the cholesterol molecule from water interactions among the considered headgroups.

Table 2 gives the number of intermolecular H-bonds and charge pairs in which the amine, intermediate groups, and choline participated. We found that H-bonds were established mostly by the unmodified amine groups, whereas in CPE-Me and CPE-Me$_2$ H-bonds with lipids were uncommon. One possible explanation for this observation is the orientation of the modified part of the headgroup: the methyl groups of CPE-Me and CPE-Me$_2$ were oriented toward the membrane core, whereas the hydrogen atoms were exposed toward the water phase. To validate this view, we calculated the distribution of the angle between the bilayer normal and the N-H and N-C bonds in the CPE-Me headgroup (Fig. 5). The N-C vector was found to have a preference for orientation toward the membrane interior (102° and 117° in CPE-Me and CPE-Me$_2$ respectively), whereas the N-H vector tended to be oriented more toward the water phase (85° and 72° in CPE-Me and CPE-Me$_2$, respectively). To explore this feature more thoroughly, we analyzed interactions of water with this part of the headgroup. First, we calculated the number of H-bonds between water and N-H groups. In this analysis we treated each hydrogen in CPE, CPE-Me, and CPE-Me$_2$ separately and found 0.458 ± 0.001, 0.528 ± 0.001, and 0.483 ± 0.001 H-bonds per N-H in CPE, CPE-Me, and CPE-Me$_2$, respectively. The lowest number for CPE resulted from the fact that the ammonium group participated in numerous H-bonds with lipids, which was not the case for CPE-Me and CPE-Me$_2$ due to the above-mentioned tendency to be oriented toward the water phase. The decrease observed for CPE-Me$_2$ compared to CPE-Me was due to a change in the charge distribution; partial charges on N and H in this group were smaller, and thus H-bonds created by this
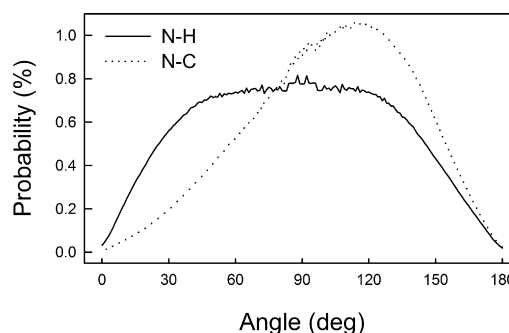

FIGURE 5 Distribution of the angle between the (outgoing) bilayer normal and the N-H (*solid*) and N-C (*dotted*) bonds in the headgroup of CPE-Me.

group were weaker. For charge pairs, we observed an increase in their number with an increasing number of methyl groups. However, if we consider the number of charge pairs per individual methyl, the order was reversed (Table 2) due to orientation of the methyl group toward the membrane.

We also analyzed the water hydrating the methyl groups in the choline and the two intermediate groups. We found that each individual methyl had 6.13 ± 0.001, 7.04 ± 0.001, and 8.16 ± 0.001 neighboring water molecules in PSM, CPE-Me$_2$, and CPE-Me, respectively. These numbers seem to contradict the above-described changes, since one would expect the methyl groups of CPE-Me$_2$ and CPE-Me that are oriented more toward the membrane to be less hydrated. However, in this case, one has to take into account the fact that these groups have a larger water-accessible surface area due to the substitution of the large methyl group by the small hydrogen. This increased hydration likely is the reason for the higher hydration of the cholesterol's hydroxyl group and the weakened water-shielding properties of the modified groups. Examples of molecular structures illustrating the above-mentioned preferences in orientation relative to the membrane normal for N(CH$_3$)$_2$H and N(CH$_3$)H$_2$ are shown in Fig. S6.

DISCUSSION

Effect of headgroup size on membrane properties in one-component bilayers

Variations in the headgroup structure of membrane lipids are huge, ranging from the small hydroxyl groups of ceramides to the large headgroups of gangliosides and globosides containing a multitude of functional groups. The headgroups affect the milieu (e.g., hydration, electrostatics, pH, and polarity) at the water-lipid interface, and also provide a highly significant means for selective interactions between membrane components, including lipid-lipid interactions and annular/non-annular lipid-protein interactions (40,41). It has been shown that the phosphocholine headgroup affects interactions with cholesterol and is a stabilizing

TABLE 2   Headgroup interactions of SM analogs

Lipids	H-bonds (N-H)	Charge pairs	H-bonded water	Water bridges
CPE	2.14	-	4.29	0.59
CPE-CHOL	2.04	-	4.68	0.65
CPE-ME	0.76	1.88 (1.88)	5.02	0.64
CPE-ME-CHOL	0.69	1.67 (1.67)	5.38	0.55
CPE-ME$_2$	0.4	2.94 (1.47)	5.19	0.64
CPE-ME$_2$-CHOL	0.36	2.58 (1.30)	5.53	0.57
PSM	-	3.83 (1.28)	5.37	0.7
PSM-CHOL	-	3.36 (1.12)	5.67	0.6

Number of intermolecular H-bonds per lipid molecule where the donor is the amine group, number of intermolecular charge pairs per lipid molecule (per methyl group), number of H-bonds between water and lipid molecules, and number of water bridges. The systems were composed of pure SM analogs and mixtures with 20 mol % cholesterol, and errors are <0.01.

factor in sterol-phospholipid interactions (19,25). SMs and PCs have the same phosphocholine headgroup but differ in their interfacial structure. In this work, the size of the headgroup was shown to affect acyl chain interactions, with a decrease in headgroup size leading to an increase in T_m (Fig. 1). In analogy, atomistic MD simulations showed that a decrease in headgroup size of the SM analogs caused an increase in membrane order due to closer molecular packing (Fig. 4). A smaller headgroup allows for closer molecular contact and increased van der Waals attractive interactions between the acyl chains, resulting in a higher membrane order and T_m. The T_m-values of the SM analogs were constantly higher than the corresponding PC analogs. The additional interfacial functional groups in SMs enable them to take part in H-bonding and charge pairing. The increased interactions at the membrane interface favor stronger van der Waals interactions between the acyl chains, and thus a higher T_m. The increased interactions at the membrane interface and subsequent increase in membrane order could also partially account for the observed increase in sterol affinity for SM analogs as compared to PC analogs.

For the SM analogs, atomistic MD simulations showed that CPE-Me and CPE-Me$_2$ display distinctly different behaviors regarding the orientation of their N-linked hydrogens and methyl groups, due to the balance of their interactions with water and the membrane region (Fig. 6). This is most evident when CPE-Me and CPE-Me$_2$ are compared with PSM. The methyl groups of PSM carry a comparatively large charge that renders the choline group water-soluble. However, the structure of the water around the choline group is clathrate-like, which is more typical for hydrophobic than hydrophilic groups (Fig. 6) (42). Meanwhile, the methyl groups of CPE-Me and CPE-ME$_2$ carry a smaller partial charge than the choline group, and thus these groups are slightly more hydrophobic. This implies that their optimal location is shifted toward the more hydrophobic interfacial region. The N-C bonds hence orient themselves toward

the membrane, whereas the N-H bonds orient toward the water phase. Consequently, the number of H-bonds involving the N-H group is largely reduced and is not compensated for by charge pairs. What also differentiates CPE-Me and CPE-Me$_2$ from PSM is the stronger hydration of the methyl groups in spite of their location. As a result of this hydration, water can more easily come into contact with the hydrophobic interior of the membrane, and we can conclude that these groups are less effective as umbrellas shielding the membrane interior from water. This may affect the overall phase behavior of these lipids and explain the observed distinctions in sterol interactions.

Effect of headgroup size on sterol affinity and membrane properties in fluid bilayers

An increase in headgroup size increased the sterol affinity for bilayers containing both SM and PC analogs (Fig. 2). Assuming an ideal mixing of POPC and the SM analogs, a larger headgroup shielded the sterol molecule from water molecules and thus also from cyclodextrin-mediated desorption to a larger extent as compared to a smaller headgroup. In addition to the decrease in molecular area (Fig. 4 A), a decrease in headgroup size also affected the positioning of the headgroup and hydration of the interface. This resulted in an even less effective shielding of the sterol molecule from unfavorable interactions with water. In agreement with this, the condensing and ordering effects of cholesterol were larger in PSM-containing bilayers as compared to the other SM analogs with smaller headgroups (Fig. 4, A–C). Sterol affinity was also considerably higher for PSM-containing bilayers at 37°C than for the other SM analogs. The effects of SM-SM and SM-POPC interactions on sterol affinity are also important if microscopic heterogeneities (not constituting a phase) are formed in the fluid phase of POPC and SM analog mixtures. A smaller headgroup allows for stronger SM-SM interactions, resulting in decreased SM-sterol interactions and a lower sterol affinity.

When comparing SM and PC analogs, sterol affinity was consistently higher for the SM analogs. Results from the MD simulations indicate that the increased possibilities for electrostatic interactions stabilized the SM-sterol interactions by allowing for the formation of H-bonds and charge pairs between the SM analogs and the hydroxyl group of cholesterol (Table 1). Increased electrostatic interactions between SM analogs and cholesterol resulted in an increased sterol affinity.
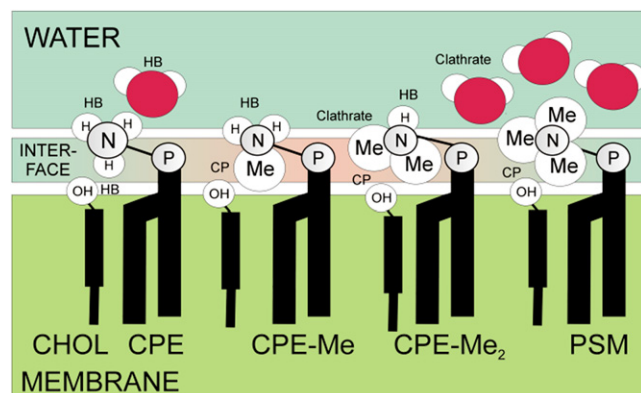

FIGURE 6 Representation of the typical interactions and orientations of the lipid headgroups of SM analogs. The figure highlights how the nature of interactions (hydrogen bond (HB) and charge pair (CP)) changes at the interfacial region as CPE is systematically changed toward PSM.

Effect of headgroup size upon the formation of ordered domains in complex lipid systems

The formation of sterol-containing ordered domains was markedly affected by the size of the SM headgroup. In lipid systems with phase separation and formation of ordered

domains, the sterol content of ordered domains is affected by several molecular interactions. In addition to SM-cholesterol interactions, SM-SM and SM-POPC interactions are important determinants of sterol content and the thermostability of ordered domains.

As demonstrated by the DPH anisotropy experiments (Fig. 1) and the MD simulations (Fig. 4), a smaller headgroup enabled a tighter molecular packing and thus a higher T_m. Regarding the molecular packing in gel-like ordered domains, it is important to emphasize that the packing can allow the presence of cholesterol, as seen for PSM, but can also be tight enough to exclude cholesterol, as seen for ceramides and glycosphingolipids (32,43). Using the anisotropy of tPa (Fig. 3 and Fig. S3) and DSC (Fig. S2), we confirmed that all of the analogs formed ordered domains in a fluid matrix in both the presence and absence of cholesterol. It is therefore likely that a decrease in headgroup size led to a tighter molecular packing and subsequent partial exclusion of sterol from the ordered domains. Among the PC analogs, DPPC and DPPE-Me$_2$ formed sterol-containing ordered domains, indicating that at least two methyl groups were needed to form sterol-containing ordered domains for the glycerol-based lipids (Fig. 3). Concerning the SM analogs, the situation was somewhat more intricate, as all analogs except CPE-Me$_2$ were able to form sterol-containing ordered domains. However, the trend was such that the saturated phospholipid analogs with larger headgroups formed domains containing more sterol as compared to analogs with smaller headgroups.

As observed from the MD simulations, the orientation of the headgroup of CPE-Me$_2$ was affected by the imbalance of having two methyl groups and one hydrogen atom in the headgroup. Together with the smaller headgroup area, the differences in orientation made the headgroup of CPE-Me$_2$ significantly worse at shielding cholesterol as compared to the choline moiety. Water interactions with cholesterol were in fact shown to be largest for CPE-Me$_2$, indicating that CPE-Me$_2$ had the lowest ability to protect cholesterol from water interactions. The headgroup orientation of CPE-Me$_2$ could also allow for differences in molecular packing of CPE-Me$_2$ affecting CPE-Me$_2$-CPE-Me$_2$ and CPE-Me$_2$-POPC interactions. A stronger association of CPE-Me$_2$ molecules in POPC mixtures could result in the formation of tightly packed gel domains with properties that would completely exclude sterols. Such gel domains could also explain the lower anisotropy of tPa in CPE-Me$_2$-containing ordered domains, since the global tPa anisotropy would be lower if tPa were excluded from the ordered domains (Fig. 3, right panels). CPE-Me$_2$ could also form very small domains that would be unable to shield CTL from quenching by 7SLPC in the quenching assay. Very small domains would be expected to be less ordered due to a disordering effect arising from the increased number of surrounding POPC molecules (in small domains, the CPE-Me$_2$ molecules interact with more POPC mole-

cules due to the longer interface). The formation of less ordered and very small domains would account for the lower molecular order, as observed with the anisotropy of tPa (Fig. 3 right panels), but cannot account for the high melting temperature of the ordered domains.

CONCLUSIONS

In this study we examined, both experimentally and by atomistic MD simulations, how the headgroup size of SM affects membrane properties and interactions with sterols. We found a clear effect of headgroup size on sterol interactions, as well as a clear difference in membrane properties and sterol interactions between SM and PC. A decrease in the headgroup size of SMs affected sterol interactions by resulting in 1), a lower ordering effect of cholesterol on the acyl chains; 2), a decrease in sterol affinity for bilayers; and 3), a decrease in the quantity of sterol in ordered domains.

The size of the headgroup affected both SM-sterol and SM-SM interactions. The increased sterol affinity for liquid-crystalline bilayers containing larger headgroup analogs can partially be explained by a larger headgroup being better able to shield sterol molecules from water interactions (24,25). However, if microscopic heterogeneities were present in the fluid phase, SM-SM interactions also affected sterol affinity. In complex lipid systems, with phase separation, the headgroup size had a marked effect on both SM-SM and SM-sterol interactions, resulting in major and varying effects on the sterol content and thermostability of ordered domains.

SUPPORTING MATERIAL

REFERENCES

1. van Meer, G., D. R. Voelker, and G. W. Feigenson. 2008. Membrane lipids: where they are and how they behave. *Nat. Rev. Mol. Cell Biol.* 9:112–124.

2. Björkqvist, Y. J., T. K. Nyholm, …, B. Ramstedt. 2005. Domain formation and stability in complex lipid bilayers as reported by cholestatrienol. *Biophys. J.* 88:4054–4063.

3. Eggeling, C., C. Ringemann, …, S. W. Hell. 2009. Direct observation of the nanoscale dynamics of membrane lipids in a living cell. *Nature.* 457:1159–1162.

4. Feigenson, G. W., and J. T. Buboltz. 2001. Ternary phase diagram of dipalmitoyl-PC/dilauroyl-PC/cholesterol: nanoscopic domain formation driven by cholesterol. *Biophys. J.* 80:2775–2788.

5. Lingwood, D., and K. Simons. 2010. Lipid rafts as a membrane-organizing principle. *Science.* 327:46–50.

6. Veatch, S. L., and S. L. Keller. 2005. Seeing spots: complex phase behavior in simple membranes. *Biochim. Biophys. Acta.* 1746: 172–185.

7. Xu, X., R. Bittman, …, E. London. 2001. Effect of the structure of natural sterols and sphingolipids on the formation of ordered sphingolipid/sterol domains (rafts). Comparison of cholesterol to plant, fungal, and disease-associated sterols and comparison of sphingomyelin, cerebrosides, and ceramide. *J. Biol. Chem.* 276:33540–33546.

8. Pike, L. J. 2006. Rafts defined: a report on the Keystone Symposium on Lipid Rafts and Cell Function. *J. Lipid Res.* 47:1597–1598.

9. Simons, K., and E. Ikonen. 1997. Functional rafts in cell membranes. *Nature.* 387:569–572.

10. Simons, K., and G. van Meer. 1988. Lipid sorting in epithelial cells. *Biochemistry.* 27:6197–6202.

11. Hancock, J. F. 2006. Lipid rafts: contentious only from simplistic standpoints. *Nat. Rev. Mol. Cell Biol.* 7:456–462.

12. Ramstedt, B., and J. P. Slotte. 1999. Interaction of cholesterol with sphingomyelins and acyl-chain-matched phosphatidylcholines: a comparative study of the effect of the chain length. *Biophys. J.* 76:908–915.

13. Smaby, J. M., H. L. Brockman, and R. E. Brown. 1994. Cholesterol's interfacial interactions with sphingomyelins and phosphatidylcholines: hydrocarbon chain structure determines the magnitude of condensation. *Biochemistry.* 33:9135–9142.

14. Björkbom, A., B. Ramstedt, and J. P. Slotte. 2007. Phosphatidylcholine and sphingomyelin containing an elaidoyl fatty acid can form cholesterol-rich lateral domains in bilayer membranes. *Biochim. Biophys. Acta.* 1768:1839–1847.

15. Martinez-Seara, H., T. Róg, …, R. Reigada. 2008. Interplay of unsaturated phospholipids and cholesterol in membranes: effect of the double-bond position. *Biophys. J.* 95:3295–3305.

16. Phillips, M. C., W. J. Johnson, and G. H. Rothblat. 1987. Mechanisms and consequences of cellular cholesterol exchange and transfer. *Biochim. Biophys. Acta.* 906:223–276.

17. Silvius, J. R., and R. N. McElhaney. 1979. Effects of phospholipid acyl chain structure on physical properties: I. Isobranched phosphatidylcholines. *Chem. Phys. Lipids.* 24:287–296.

18. Aittoniemi, J., P. S. Niemelä, …, I. Vattulainen. 2007. Insight into the putative specific interactions between cholesterol, sphingomyelin, and palmitoyl-oleoyl phosphatidylcholine. *Biophys. J.* 92:1125–1137.

19. Björkbom, A., T. Yamamoto, …, J. P. Slotte. 2008. Importance of the phosphocholine linkage on sphingomyelin molecular properties and interactions with cholesterol; a study with phosphate oxygen modified sphingomyelin-analogues. *Biochim. Biophys. Acta.* 1778:1501–1507.

20. Pasenkiewicz-Gierula, M., T. Róg, …, A. Kusumi. 2000. Cholesterol effects on the phosphatidylcholine bilayer polar region: a molecular simulation study. *Biophys. J.* 78:1376–1389.

21. Róg, T., and M. Pasenkiewicz-Gierula. 2006. Cholesterol-sphingomyelin interactions: a molecular dynamics simulation study. *Biophys. J.* 91:3756–3767.

22. Térová, B., R. Heczko, and J. P. Slotte. 2005. On the importance of the phosphocholine methyl groups for sphingomyelin/cholesterol interactions in membranes: a study with ceramide phosphoethanolamine. *Biophys. J.* 88:2661–2669.

23. Niemelä, P., M. T. Hyvönen, and I. Vattulainen. 2004. Structure and dynamics of sphingomyelin bilayer: insight gained through systematic comparison to phosphatidylcholine. *Biophys. J.* 87:2976–2989.

24. Huang, J., and G. W. Feigenson. 1999. A microscopic interaction model of maximum solubility of cholesterol in lipid bilayers. *Biophys. J.* 76:2142–2157.

25. Huang, J., J. T. Buboltz, and G. W. Feigenson. 1999. Maximum solubility of cholesterol in phosphatidylcholine and phosphatidylethanolamine bilayers. *Biochim. Biophys. Acta.* 1417:89–100.

26. Anderson, T. G., and H. M. McConnell. 2002. A thermodynamic model for extended complexes of cholesterol and phospholipid. *Biophys. J.* 83:2039–2052.

27. Somerharju, P., J. A. Virtanen, …, M. Hermansson. 2009. The superlattice model of lateral organization of membranes and its implications on membrane lipid homeostasis. *Biochim. Biophys. Acta.* 1788:12–23.

28. Gagné, J., L. Stamatatos, …, J. R. Silvius. 1985. Physical properties and surface interactions of bilayer membranes containing N-methylated phosphatidylethanolamines. *Biochemistry.* 24:4400–4408.

29. Kusube, M., H. Matsuki, and S. Kaneshina. 2005. Thermotropic and barotropic phase transitions of N-methylated dipalmitoylphosphatidylethanolamine bilayers. *Biochim. Biophys. Acta.* 1668:25–32.

30. Mason, J. T., and T. J. O'Leary. 1990. Effects of headgroup methylation and acyl chain length on the volume of melting of phosphatidylethanolamines. *Biophys. J.* 58:277–281.

31. Yu, H., and S. W. Hui. 1992. Methylation effects on the microdomain structures of phosphatidylethanolamine monolayers. *Chem. Phys. Lipids.* 62:69–78.

32. Nyholm, T. K., P. M. Grandell, …, J. P. Slotte. 2010. Sterol affinity for bilayer membranes is affected by their ceramide content and the ceramide chain length. *Biochim. Biophys. Acta.* 1798:1008–1013.

33. Silvius, J. R. 1991. Thermotropic properties of phospholipid analogues. *Chem. Phys. Lipids.* 57:241–252.

34. Koynova, R., and M. Caffrey. 1998. Phases and phase transitions of the phosphatidylcholines. *Biochim. Biophys. Acta.* 1376:91–145.

35. de Almeida, R. F., A. Fedorov, and M. Prieto. 2003. Sphingomyelin/phosphatidylcholine/cholesterol phase diagram: boundaries and composition of lipid rafts. *Biophys. J.* 85:2406–2416.

36. Halling, K. K., B. Ramstedt, …, T. K. Nyholm. 2008. Cholesterol interactions with fluid-phase phospholipids: effect on the lateral organization of the bilayer. *Biophys. J.* 95:3861–3871.

37. de Almeida, R. F., L. M. Loura, …, M. Prieto. 2002. Nonequilibrium phenomena in the phase separation of a two-component lipid bilayer. *Biophys. J.* 82:823–834.

38. Martinez-Seara, H., T. Róg, …, I. Vattulainen. 2008. Influence of cis double-bond parametrization on lipid membrane properties: how seemingly insignificant details in force-field change even qualitative trends. *J. Chem. Phys.* 129:105103.

39. Aittoniemi, J., T. Róg, …, I. Vattulainen. 2006. Tilt: major factor in sterols' ordering capability in membranes. *J. Phys. Chem. B.* 110: 25562–25564.

40. Boggs, J. M. 1987. Lipid intermolecular hydrogen bonding: influence on structural organization and membrane function. *Biochim. Biophys. Acta.* 906:353–404.

41. Lee, A. G. 2004. How lipids affect the activities of integral membrane proteins. *Biochim. Biophys. Acta.* 1666:62–87.

42. Pasenkiewicz-Gierula, M., Y. Takaoka, …, A. Kusumi. 1999. Charge pairing of headgroups in phosphatidylcholine membranes: a molecular dynamics simulation study. *Biophys. J.* 76:1228–1240.

43. Maunula, S., Y. J. Björkqvist, …, B. Ramstedt. 2007. Differences in the domain forming properties of N-palmitoylated neutral glycosphingolipids in bilayer membranes. *Biochim. Biophys. Acta.* 1768:336–345.